

---

# Luminescence from $\beta$ -Irradiated Graphene Layers

A. CHRUŚCIŃSKA\*, K.R. PRZEGIĘTKA, P. SZROEDER,  
H.L. OCZKOWSKI AND F. ROZPŁOCH

Institute of Physics, Nicolaus Copernicus University  
Grudziądzka 5, 87-100 Toruń, Poland

*(Received February 16, 2006; revised version May 4, 2006)*

We found that  $\beta$ -irradiated samples of crystallite graphite and multi-walled carbon nanotubes emit light during heating above room temperature. This behaviour is rather surprising for semimetals. Due to the lack of deep enough energy gap, this optical emission cannot be associated with interband transitions, as it is usually assumed in a thermally stimulated luminescence model. We suppose that the reported accumulated luminescence is the result of thermally stimulated relaxation of some kind of defects created in graphene structures by ionising radiation and therefore we offer to name it the relaxoluminescence. We anticipate the relaxoluminescence to be a starting point for developing a new spectroscopic method for nanotechnology. It can also throw a new light on the nature of defects, which are suspected of being responsible for strange magnetic effects in carbon.

PACS numbers: 77.60.Kn, 78.60.-b, 78.67.Ch, 81.05.Uw

## 1. Introduction

The phenomenon of thermally stimulated emission (TSE) is considered to be a process characteristic of non-metals and to be caused by recombination of electrons thermally excited from trapping levels [1]. We show here that TSE can be observed in semimetals and that  $\beta$ -irradiated graphite and multi-walled carbon nanotubes (MWNTs) emit light during heating above room temperature. We conclude that there are TSE centres in the graphene structure, where light can be produced as a result of electron transitions between localised states. Activation energy of the process is of the order of 1 eV, which is close to activation energy for defect relaxation in graphite [2]. In our opinion, relaxations of some kind of defects created in graphene layers by  $\beta$ -radiation can lead to TSE production. To

---

\*corresponding author; e-mail: alicja@phys.uni.torun.pl

distinguish the observed phenomenon from TSE found in non-metals, we suggest to call it the relaxoluminescence (RXL).

Electron or ion irradiation produces lattice disorder, which alters physical properties of graphite and carbon nanotubes. Structural defects, such as interstitial atoms, vacancies, and their aggregates, Frenkel pairs, and pentagon–heptagon pairs store the so-called Wigner energy previously deposited by ionising radiation [3]. This energy can be released by defect transformation into configurations of lower energy. Different defect rearrangement processes have various activation energies and are stimulated during annealing at various temperatures [4].

Specific types of graphene network are nanotube tips. Theoretical calculations together with tunneling microscopy measurements show that the local density of states at the tip of nanotubes presents sharp localized states with well-defined energy [5]. The luminescence produced by electronic transitions between these levels was observed during electron field emission [6]. This phenomenon provoked a simple test to see whether optical emission can be observed during the thermal annealing of graphene network with defects generated by ionising radiation.

## 2. Experimental

The multi-walled carbon nanotubes were produced by arc discharge of graphite electrodes in He gas at 500 Torr. The arc was maintained by 50 A discharge current at 21 V. MWNTs grew on the tip of the cathode during condensation of carbon plasma. For the presented studies, soft core of the cathode deposit containing nanotubes was carefully scrapped. To remove carbon nanoparticles and amorphous carbons, crude material was heated at 650°C in a flow of dry air until 95% of host material was burned. SEM and TEM images of the purified samples displayed loosely packed pillars 50  $\mu\text{m}$  in diameter and 1 mm in length which were made up of straight, rigid MWNTs. Raman spectra exhibited a sharp *G*-line accompanying a very weak *D*-peak. The detailed characteristics of samples is described elsewhere [7].

For thermally stimulated optical emission experiments, aliquots of 5 mg samples were prepared on thin nickel discs. Aliquots of MWNTs samples consisted of loosely packed pieces differing much in shape and dimensions. In case of HOPG (Union Carbide Corporation UCAR, ZYB quality) we used single pieces of rectangular shape and a thickness of about 0.5 mm.

All the glow curves as well as the isothermal decay measurements were obtained using the commercial Risø OSL-TL-DA-12 System [8], which is widely used in luminescence dosimetry. Excitation was carried out by  $^{90}\text{Sr}/^{90}\text{Y}$  radioactive source incorporated in Risø System. The activity of  $^{90}\text{Sr}$  is 1.16 GBq. The calibration of the dose rate was carried out on quartz grain samples producing a result of 50 mGy  $\text{s}^{-1}$ . This value could also be used as a rough estimate for carbon structures studied here. The absorbed dose mainly originates from  $\beta$  radiation, but it contains also a component related to  $\gamma$  radiation. The exact value of the absorbed

dose in some extent depends on the material composition and, for MWNT and graphite samples, the doses can be delivered at a slightly different rate than for quartz. The average energy of  $\beta$  particles emitted by the  $^{90}\text{Sr}$  source is 0.196 MeV for which the range in graphite is *ca.* 300  $\mu\text{m}$ . Due to loose packing structure of nanotube bundles, the expected range in MWNT should exceed that of graphite.

Heating was realized in pure argon flow immediately after irradiation. The heating rate was 5 K/s. All the presented results of emission measurement were obtained using a wide band filter BG-39 with the transmission window extending from 340 nm to 610 nm (3.6–2.0 eV). However, the emission was also observed with a near UV filter U-340 with transparency window 290–370 nm (4.28–3.35 eV), but signal intensity was much lower and it needed a far longer irradiation to be detected. This suggests that either the emission spectrum depends on the defect concentration or the emission band lies near the low energy edge of U-340 filter and the tail of emission is observed for higher intensities.

### 3. Results and discussion

To induce structural defects, samples of highly oriented pyrolytic graphite (HOPG) and MWNT were exposed several times to doses of 90 Gy of  $\beta$ -rays. After each irradiation, light emission during linear heating from room temperature up to 500°C was detected. Repeated heating without prior irradiation produced only incandescence, which revealed a transient character of the emission and indispensable role of irradiation in the phenomenon. Series of the glow curves obtained during successive irradiation-heating cycles are presented in Fig. 1. For both samples the pre-dose effect, which consists of the emission intensity increase after each

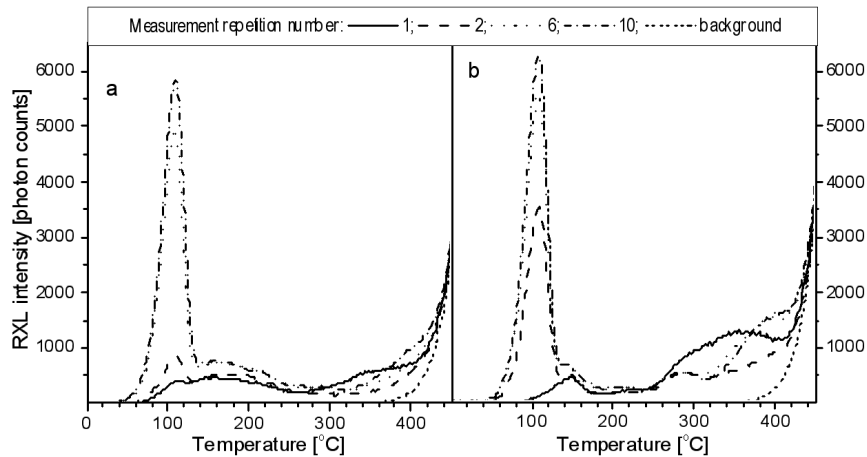


Fig. 1. Emission measured during the heating of MWNTs (a) and HOPG (b) samples. Each sample was repeatedly subjected to 90 Gy dose of  $\beta$  radiation and subsequent heating. The curve “background” was measured without prior irradiation immediately after the first glow curve registration. Pre-dose effect appears manifestly for the peak at 108°C.

cycle of irradiation and heating, has been recognised for the registered curves in the whole temperature range. In particular, the main peak at 108°C reveals this effect emphatically.

Although, the results for two samples (one for MWNTs and one for HOPG) are presented in Fig. 1, we actually obtained repeatable glow curves for 8 individual samples. We excluded artificial source of measured signals (like apparatus effects, contaminations, etc.). We also checked that pure amorphous carbon samples gave no rise for luminescence signal.

The features of thermally stimulated process (TSP) are reflected by the shape of glow curves. Hence, one can attempt a conventional glow curve shape analysis, as it is used in standard TSE studies [1]. For the graphite sample with an absorbed dose of 135 Gy the most intensive peak of RXL resides at 108°C (Fig. 2). Its shape

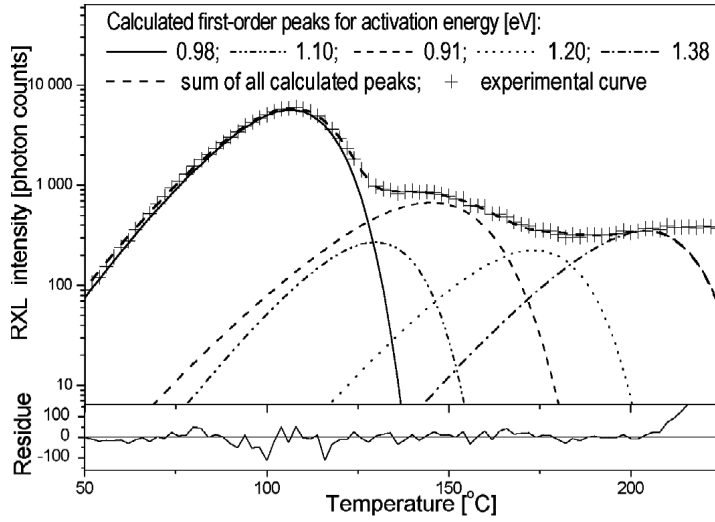


Fig. 2. Examples of the fitting procedure results for HOPG after irradiation with the dose of 135 Gy. The difference between the experimental data and the sum of all components is presented in the bottom inset.

indicates that the observed emission is produced by the first-order kinetic process described by [9]:

$$I(T) = n_0 s \exp\left(-\frac{E}{kT}\right) \exp\left(-\frac{s}{\beta} \int_{T_0}^T \exp\left(-\frac{E}{kT'}\right) dT'\right), \quad (1)$$

where  $I$  is the emission intensity,  $T$  is the temperature,  $k$  is Boltzmann's constant,  $n_0$  denotes the initial concentration of defects which take part in the RXL process,  $s$  is called the pre-exponential or frequency factor,  $E$  is the activation energy, and  $\beta$  is the heating rate. Fitting of (1) to the above-mentioned peak gives:  $E_1 = 0.980 \pm 0.02$  eV and  $s_1 = 4.1 \pm 2.3 \times 10^{12}$  s<sup>-1</sup>. A similar analysis of the RXL peak at 108°C for MWNT sample yields exactly the same set of values ( $E_1, s_1$ ).

In the glow curves four additional maxima can be distinguished at 145°C, 205°C, 285°C, and 345°C (Fig. 1). These peaks are difficult to analyse due to weak intensities and overlap effects. However, the MWNT sample, after absorbing the dose of 270 Gy, shows a clear RXL maximum at 145°C. Its main component can be fitted nicely by formula (1) resulting in  $E_2 = 0.91 \pm 0.02$  eV and  $s_2 = 13.3 \pm 1.7 \times 10^{10}$  s<sup>-1</sup>.

The quality of the glow curve fitting procedure was controlled by minimisation of the residue, i.e. the difference between the calculated (simulated) and measured emission intensity for every point of the glow curve. The course of residue value is presented on the bottom of Fig. 2. For the best fit we found:  $E_1 = 0.980$  eV and  $s_1 = 4.1 \times 10^{12}$  s<sup>-1</sup>, while the maximal value of residue in the temperature range of the main peak (70–140°C) is never higher than 3% of the current emission intensity. It should be stressed that the fitting results were very sensitive to changes of parameter values ( $E$  and  $s$ ). We observed that when the deviation from the determined  $E_1$  value reached 0.01 eV it produced a considerable increase in the residue amplitude. Moreover, reducing the level of residue by changing the pre-exponential factor  $s$  was impossible due to the strong dependence of the peak width on both parameters values. On the other hand, the accuracy of temperature control in our equipment is not better than 2°C. This is supposed to be the main source of uncertainty of the energy value  $E$ . In order to estimate the influence of temperature  $T$  on the fitting results, the registered curve was shifted by  $-2^\circ\text{C}$  towards lower temperature and the fitting procedure was repeated. This way we obtained the lowest possible values of energy and the pre-exponential factor:  $E_{L1} = 0.96$  eV and  $s_{L1} = 1.8 \times 10^{-12}$  s<sup>-1</sup>. Analogously, shifting the glow curve for  $+2^\circ\text{C}$  gave maximal values for the energy and the pre-exponential factor:  $E_{H1} = 1.00$  eV and  $s_{H1} = 6.4 \times 10^{-12}$  s<sup>-1</sup>. The fitting quality of the shifted curves was the same as in the case of the original one. These two pairs of limits allowed us to establish the range of the most probable values:  $E_1 = 0.980 \pm 0.02$  eV and  $s_1 = 4.1 \pm 2.3 \times 10^{12}$  s<sup>-1</sup>. The uncertainties for parameters characterising RXL peak at 145°C ( $E_2$ ,  $s_2$ ) were estimated in the same way. Other glow curve maxima are not well separated and the values of their parameters cannot be determined as sharp as in the case of the main peak. Hence, in Fig. 2 we presented only rough approximations of the activation energy related to further peaks arising in the glow curves.

The expression:  $s \exp(-E/kT)$  in (1) determines the probability rate  $\nu$  of a single defect taking part in the RXL process. Hence, at a definite temperature  $T$  the lifetime of a particular type of defect undergoing the TSP can be calculated using:

$$\tau = \frac{1}{s} \exp\left(\frac{E}{kT}\right). \quad (2)$$

Bearing this in mind, it is clear that for an irradiated sample kept at a constant temperature the plot of RXL light intensity vs. annealing time should

decay exponentially. This is the basic idea behind the experimental technique, usually called isothermal decay (ID). We applied it to confirm the values of  $E$  and  $s$  estimated by the glow curve fitting.

The measurements were carried out at four temperatures  $T_{\text{iso}}$ : 30°C, 50°C, 70°C, and 90°C. The detailed results are showed in Fig. 3 and for a better comparison of particular curves are once more redrawn in Fig. 4.

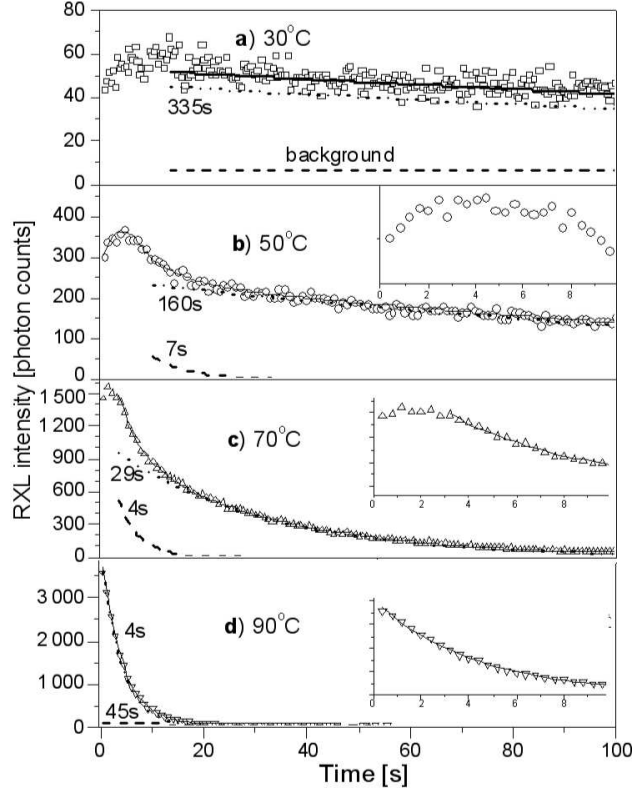


Fig. 3. The detailed results of fitting of the isothermal decay curves (represented by symbols) for MWNTs sample. Next to the plot of particular component, its value of the time constant  $\tau$  is printed. The solid line represents the sum of both components. Inset panels focus on the initial behaviour of the RXL.

It is noticeable that except the case of  $T_{\text{iso}} = 90^\circ\text{C}$  the initial (limited only to the first few seconds of annealing) increase in the registered RXL intensity takes place. We suppose, this is caused by some process competing with the relaxation responsible for luminescence.

Anyway, a nonlinear least squares method was applied to fit two-exponential decay function to the declining part of the ID curve:

$$Y(t) = y_0 + A_1 \exp\left(\frac{-t}{\tau_1}\right) + A_2 \exp\left(\frac{-t}{\tau_2}\right), \quad (3)$$

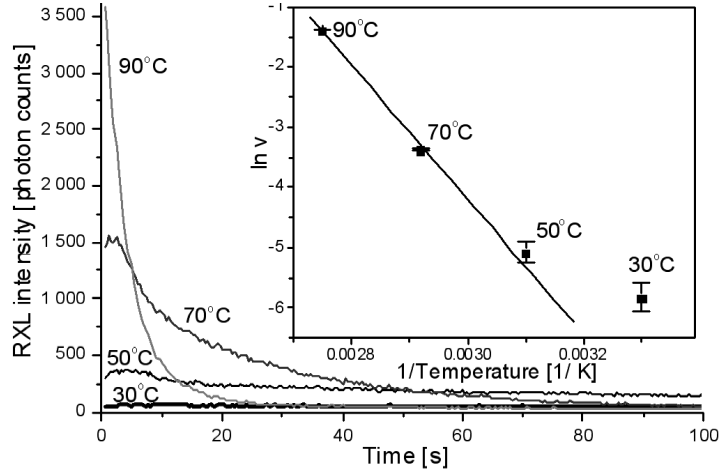


Fig. 4. The isothermal decay results obtained at four temperatures and *Arrhenius* plot (inset) for MWNTs sample. The declining parts of the isothermal curves were fitted by the two-exponential decay function. The decay rate values ( $\nu = 1/\tau$ ) of the main components were used for the construction of *Arrhenius* plot, where error bars denote standard errors. The linear regression to the *Arrhenius* plot gave the value of the activation energy  $E$ . The point representing the decay rate value  $\nu$  at 30°C was not used for linear regression. In our opinion, the faster decay at lower temperature results in the observed effect of anomalous fading.

where  $Y$  is the ID emission intensity,  $t$  — the annealing time,  $y_0$  — background signal,  $A_i$  — the  $i$ -component intensity and  $\tau_i$  — the decay time constant of  $i$ -component.

Figure 3a reveals a very poor fitting for ID curve recorded at  $T_{\text{iso}} = 30^\circ\text{C}$ , where the lowest RXL intensity was strongly influenced by background. The decay rate  $\nu$  was calculated as the reciprocal of the time constant  $\tau$  expressed in seconds.

The decay rate values of the main (dominating) component of the function (3) were considered for constructing the *Arrhenius* plot (inset in Fig. 4). The values of  $(\ln \nu)$  were plotted versus the reciprocal temperature  $T_{\text{iso}}$  (termed in K). The error bars denote standard errors. As it is easily noticeable the point representing  $T_{\text{iso}} = 30^\circ\text{C}$  does not follow the linear trend of the other ones, but, as we suppose, this is the result of poor detection of the main component at this temperature. Then weighted linear regression was applied only to the three other points (obtained for  $T_{\text{iso}}$  of  $90^\circ\text{C}$ ,  $70^\circ\text{C}$ , and  $50^\circ\text{C}$ ). For both the MWNT and the graphite samples the results of ID experiments were very similar:  $E_{1d} = 0.97 \pm 0.07$  eV with  $s_{1d} \approx 10^{13} \text{ s}^{-1}$  and  $E_{1d} = 0.98 \pm 0.08$  eV with  $s_{1d} \approx 10^{13} \text{ s}^{-1}$ , respectively for MWNT and HOPG samples, where maximal errors calculated by partial derivatives method are given as uncertainties. Hence, we present here only data obtained for the MWNT sample, Figs. 3 and 4.

TABLE  
The decay time of RXL peaks at 108°C and 145°C.

Sample temperature (°C)	Life time of defects	
	RXL peak at 108°C ( $E_1, s_1$ )	RXL peak at 145°C ( $E_2, s_2$ )
20	5 h	9.5 h
30	1.5 h	3 h
50	8 min	20 min
70	1 min	3 min
90	10 s	33 s

The values of lifetime at different temperatures for two main RXL peaks obtained from (2) are collected in Table. As a matter of fact, these values can be estimated also by comparing the glow curve intensities measured before and after isothermal experiments (taking into account the pre-dose effect). Anyway, the observed decay of RXL signal seems to be a faster than it is suggested by the results presented in Table. The reason could be the existence of an additional channel of recombination, which is more efficient in lower temperatures.

#### 4. Conclusions

Although the mechanism of the observed light production is not quite clear, our results prove that it is a kind of accumulated luminescence. We proposed to call it the relaxoluminescence (RXL), because of its obvious connection with defects relaxation and to distinguish it from thermoluminescence (TL) observed in non-metals. However, in order to characterize RXL, we applied experimental techniques and nomenclature developed and typically used for investigation of TL in isolators and semiconductors [10–22].

We assume that each pair of parameters  $E$  and  $s$  yielding a single peak in the glow curve is connected with a single type of defect taking part in the RXL process. Hence, the shape of glow curves reveals information on the spectrum of defects in the sample. The positions of maxima in glow curves are similar for both MWNT and HOPG samples and they remain stable regardless of the number of excitation-heating cycles and the value of absorbed dose. The relative intensities of particular peaks, however, depend on the absorbed dose, the history of the excitation-heating cycles, and also vary from sample to sample. Hence, RXL measurements can act as a convenient tool for controlling the density of defects of particular type in graphene structures.

So far, visible luminescence in metals has been observed only during field emission experiments. The light emission is then caused by recombination of electron-hole pairs, which are created on semiconducting inclusions by ionization of atoms by the acceleration of conduction electrons [23]. Such phenomenon has



also been observed on the etched carbon fibres. In this case the luminescence spectrum contains two peaks at 2.17 and 2.48 eV [24]. In experiments with field emission from semimetallic MWNT, the peak extending from 1.5 to 2.5 eV has been detected [6]. One can speculate that RXL, which we observe in the range of  $2.0 \div 3.6$  eV, become possible only when localized states related to deformed graphene network emerge. As a matter of fact, we do not exactly know what is the origin of these states. RXL spectroscopy should bring more information. Unfortunately, due to low intensity and transient character of the emission we were not able to record luminescence spectra in our laboratory.

One should emphasize that activation energy of 0.98 eV of light emission at 108°C is close to activation energy of disorder-induced *D* line decay (0.89 eV) obtained in Raman experiments with irradiated graphite [2]. The RXL maximum recorded at 205°C can be related to the Wigner energy release peak observed in the calorimetric experiments [4, 25, 26]. At this stage of investigation, however, the role of defect relaxation in emission production is not clear. Neither the way of energy transfer from relaxation process to light emission, nor the electron states between which the optical transitions take place, can be indicated. The advanced techniques of atomic and electronic structures investigation such as high-resolution transmission electron microscopy (HRTEM), electron spin resonance (ESR), Raman spectroscopy applied simultaneously with TSE measurements can bring some new information into this subject.

Our observation is parallel to some recent reports on magnetic ordering in some carbon materials [27]. This effect is also transient and is caused by defects. Probably, in both relaxoluminescence and magnetic ordering phenomena, defects of the same kind take part.

As a matter of fact, TL phenomenon was for the first time observed exactly in carbon — Sir Robert Boyle discovered it in diamond and reported to the Royal Society in London in 1663 (R. Boyle, *Experiments and Considerations upon Colours with Observations on a Diamond that Shines in the Dark*, Henry Herringham, London 1664). However, accumulated luminescence was never expected to occur in graphite and its derivatives. The presented results obtained for both HOPG and MWNT are uniform, which suggests that RXL is a common feature of carbon forms with a small energy gap and the related processes take place in graphene layers.

### Acknowledgments

We thank Dr. M. Michalski for help. This work has been supported by N. Copernicus University grant No. 446-F.

### References

- [1] S.W.S. McKeever, R. Chen, *Theory of Thermoluminescence and Related Phenomena*, World Scientific, Singapore 1997.
- [2] E. Asari, M. Kitajima, K.G. Nakamura, *Phys. Rev. B* **47**, 11143 (1993).

- [3] F. Banhart, *Rep. Prog. Phys.* **62**, 1181 (1999).
- [4] T. Iwata, *J. Mater. Nucl.* **133-134**, 361 (1985).
- [5] D.L. Carroll, P. Redlich, P.M. Ajayan, J.C. Charlier, X. Blasé, A. De Vita, R. Car, *Phys. Rev. Lett.* **78**, 2811 (1997).
- [6] J.M. Bonard, T. Stöckli, F. Maier, W.A. de Heer, A. Châtelain, *Phys. Rev. Lett.* **81**, 1441 (1998).
- [7] P. Szroeder, W. Marciniak, F. Rozpłoch, *Solid State Phenomena* **94**, 275 (2003).
- [8] L. Botter-Jensen, G.A.T. Duller, N.R.J. Poolton, *Rad. Meas.* **22**, 549 (1992).
- [9] J.T. Randall, M.H.F. Wilkins, *Proc. R. Soc. Lond. A* **184**, 366 (1945).
- [10] H.L. Oczkowski, *J. Lumin.* **17**, 113 (1978).
- [11] H.L. Oczkowski, A. Pietkun, *J. Lumin.* **59**, 65 (1994).
- [12] A. Chruścińska, H.L. Oczkowski, K. Przegiętka, *Opt. Appl.* **25**, 273 (1995).
- [13] A. Chruścińska, H.L. Oczkowski, K. Przegiętka, *Acta Phys. Pol. A* **89**, 555 (1996).
- [14] A. Chruścińska, *J. Lumin.* **62**, 115 (1994).
- [15] A. Chruścińska, H.L. Oczkowski, K. Przegiętka, *J. Lumin.* **72-74**, 648 (1997).
- [16] A.J. Wojtowicz, J. Glodo, W. Drozdowski, K.R. Przegietka, *J. Lumin.* **79**, 275 (1998).
- [17] A.J. Wojtowicz, W. Drozdowski, D. Wiśniewski, K. Wiśniewski, K. Przegiętka, H.L. Oczkowski, T.M. PETERS, *Rad. Meas.* **29**, 323 (1998).
- [18] M. Załęski, M.T. Borowiec, H. Szymczak, K. Przegiętka, H.L. Oczkowski, *Opt. Commun.* **151**, 46 (1998).
- [19] K. Przegiętka, H.L. Oczkowski, Fr. Rozpłoch, W. Drozdowski, K. Fabisiak, in: *Science and Technology of Carbon - EuroCarbon'98, Strasbourg 5-9 July 1998, Extended Abstracts and Programme*, Vol. II, 893 (1998).
- [20] W. Drozdowski, K. Przegiętka, A.J. Wojtowicz, H.L. Oczkowski, *Acta Phys. Pol. A* **95**, 251 (1999).
- [21] L. Duggan, M. Budzanowski, K. Przegiętka, N. Reitsema, J. Wong, T. Kron, *Rad. Meas.* **32**, 335 (2000).
- [22] A. Chruścińska, H.L. Oczkowski, K.R. Przegiętka, *J. Phys. D, Appl. Phys.* **34**, 2939 (2001).
- [23] R.E. Hurley, P.J. Dooley, *J. Phys. D, Appl. Phys.* **10**, 195 (1977).
- [24] R.V. Latham, D.A. Wilson, *J. Phys. D, Appl. Phys.* **14**, 2139 (1981).
- [25] E.W. Mitchell, M.R. Taylor, *Nature* **208**, 638 (1965).
- [26] C.P. Ewels, R.H. Telling, A.A. El-Barbary, M.I. Heggie, *Phys. Rev. Lett.* **91**, 25505 (2003).
- [27] A.V. Rode, E.G. Gamaly, A.G. Christy, J.G. Fitz Gerald, S.T. Hyde, R.G. Elliman, B. Luther-Davies, A.I. Veinger, J. Androulakis, J. Giapintzakis, *Phys. Rev. B* **70**, 054407 (2004).